Novel Cyano- and Amidinobenzothiazole Derivatives: Synthesis, Antitumor Evaluation, and X-ray and Quantitative Structure−Activity Relationship (QSAR) Analysis

Irena Ćaleta,[†,§] Marijeta Kralj,*[,‡] Marko Marjanović,[‡] Branimir Bertoša,[#] Sanja Tomić,[#] Gordana Pavlović,[⊥] Krešimir Pavelić,[‡] and Grace Karminski-Zamola*[,†]

Department of Organic Chemistry, Faculty of Chemical Engineering and Technology, University of Zagreb, Marulićev trg 20, P.O. Box 177, HR-10000 Zagreb, Croatia, Division of Molecular Medicine and Division of Physical Chemistry, Ruđer Bošković Institute, Bijenička cesta 54, P.O. Box 1016, HR-10000 Zagreb, Croatia, and Faculty of Textile Technology, University of Zagreb, Prilaz baruna Filipovića 28a, HR-10000, Zagreb, Croatia

Received December 11, 2008

Synthesis of a series of novel cyano- and amidinobenzothiazole derivatives **3**−**31** is described. All studied amidino derivatives showed noticeable antiproliferative effect on several tumor cell lines. Cyano derivatives **11**−**17** showed considerably less pronounced activity because of their poor solubility in aqueous cell culture medium, which was confirmed by the principal components (PC) analysis. Compounds **21**, **22**, **28**, and **29** were tested for their effects on the cell cycle and apoptosis, whereby **22** and **29**, having methyl group at the C-6 position in pyridine ring, showed drastic cell cycle perturbations that were both concentration- and time-dependent and induced apoptosis. The QSAR modeling, based on the physicochemical descriptors and on the measured biological activities, indicated the relevance of molecular polarizability and particular distribution of pharmacophores on the molecular surface for activity. In conclusion, benzothiazoles containing either isopropylamidino or imidazolyl groups will be considered as starting compounds for further investigation on lead identification.

Introduction

Despite major breakthroughs in diagnosis and treatment, cancer is still the second leading cause of death in the Western world. The discovery and development of new, more active, more selective, and less toxic compounds for the treatment of malignancy are one of the most important goals in medicinal chemistry. The understanding of the fundamental biology of cancer increased dramatically in recent years[1] and has strongly impacted both experimental and clinical tumor therapy. It is believable that the future of tumor therapy is in the development of molecularly targeted agents that specifically block key mechanisms involved in development and progression of specific types of cancer.[2] Two potential targets for drug design in cancer are DNA and different types of proteins like kinases or topoisomerase I/II. The design of new intercalators[3,4] and groove-binders[5,6] and the discovery of specific protein inhibitors[4,7,8] are two important approaches in the search of new chemoterapeutic agents.

Since the 1990s, various pharmacological investigations of newly synthesized benzothiazoles demonstrated interesting pharmacological activities and led to development of new medications for treating diseases. They were studied extensively for their antiallergic,[9] anti-inflammatory,[9,10] antitumor[11−14] and analgesic activity.[15,16] Apart from the above mentioned activities, benzothiazole derivatives also showed some interesting efficacy as kinase,[17−20] topoisomerase I/II[21,22] and trans-retinoic acid metabolism[23,24] inhibitors. Therefore, various benzothiazole compounds are of considerable interest for their diverse pharmaceutical uses and play a vital role in the synthesis of fused heterocyclic systems.

The above considerations prompted us to design and synthesize a new series of cyano- and amidino-substituted benzothiazole derivatives (Figure 1) and to test their antiproliferative activity of tumor cells in vitro. In order to find out which chemical and physical descriptors are most relevant for inhibition of the specific cell lines growth, we derived the Volsurf parameters and, using PLS[a] statistical analysis, we determined the relationship between these descriptors and molecular activities. In this way, QSAR models were derived for several tested cell lines.

Chemistry

All compounds (**3**−**31**) shown in the Figure 1 were prepared according to the Schemes 1 and 2, starting from commercially available 4-aminobenzonitrile. 2-Amino-6-cyanobenzothiazole **1** was obtained using a slightly changed conventional procedure with potassium thiocyanate and HCl(conc)/H_2O in a two-step synthesis.[25,26] Cyano-substituted benzamides **3**−**6** were prepared by a published method.[27] Compound **1** was also treated with

* To whom correspondence should be addressed. For M.K.: phone, +385 1 4571 235; fax, +3851 4561 010; e-mail, marijeta.kralj@irb.hr. For G.K.-Z.: phone, ++38514597215; fax, ++38514597250; e-mail, gzamola@fkit.hr.

† Faculty of Chemical Engineering and Technology, University of Zagreb.

§ Current address: GlaxoSmithKline Research Center Zagreb Limited, Prilaz baruna Filipovića 29, HR-10000 Zagreb, Croatia.

‡ Division of Molecular Medicine, Ruđer Bošković Institute.

Division of Physical Chemistry, Ruđer Bošković Institute.

⊥ Faculty of Textile Technology, University of Zagreb.

[a] Abbreviations: 7-AAD, 7-amino-actinomycin D; DMEM, Dulbecco's modified Eagle medium; DMSO, dimethyl sulfoxide; FBS, fetal bovine serum; H 460, lung carcinoma; HAS, hydrophobic surface area; HeLa, cervical carcinoma; Hep-2, laryngeal carcinoma; LOO, Leave-One-Out; LV, latent variables; MCF-7, breast carcinoma; MiaPaCa-2, pancreatic carcinoma; MIF, molecular interaction fields; MTT, 3-(4,5-dimethylthiazole-2-yl)-2,5-diphenyl tetrazolium bromide; OD, optical density; PBS, phosphate buffered saline; PG, percentage of growth; PI, propidium iodide; PC, Principal Components; PLS, Partial Least Square; QSAR, Quantitative Structure Activity Relationship; SDEP, standard deviation of the error of prediction; SW 620, colon carcinoma; VD, a measure of relative partition of compounds between plasma and tissue; W, volume of water molecule; WI 38, diploid fibroblasts; WN, volume of amide molecule; WO, volume of the oxygen probe.

10.1021/jm801566q CCC: $40.75
Published on Web 03/05/2009

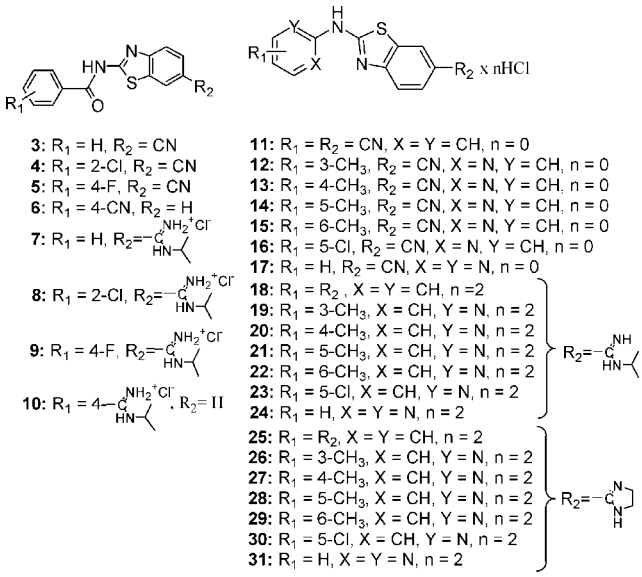

Figure 1. Substituted cyano- and amidinobenzothiazole derivatives (**3**−**31**).

copper(II) bromide and *tert*-butyl nitrite in acetonitrile to form the corresponding 2-bromo-6-cyanobenzothiazole **2**. Compound **2** served as an intermediate for the synthesis of novel cyano derivatives of 2-(hetero)arylaminobenzothiazole **11**−**17**. Novel amidinobenzothiazole derivatives **7**−**10** and **18**−**31** were prepared by the classical Pinner reaction[28] from cyano derivatives (**3**−**6**, **11**−**17**).

Molecular and Crystal Structure of Compound 15

The ORTEP-3 (version 1.08)[29] drawing of the molecular structure of compound **15** is depicted in Figure 2a and its crystal structure in Figure 2b. The molecule is not essentially planar in the crystalline state. The dihedral angle between planes defined by the atoms of pyridine and benzothiazole ring amounts to 5.68(8)°.

The rings bond lengths are normal. The thiazole ring C1−N1 bond length (1.313(2) Å) is shorter then N1−C2 (1.382(2) Å). The bond lengths between the sulfur and the carbons of the thiazole ring are 1.741(2) Å (S1−C7) and 1.751(2) Å (S1−C1). The N2−C1 (1.359(3) Å) and N2−C8 (1.393(2) Å) bonds are delocalized within the π-electron system of pyridine and the benzothiazole ring.

The molecules are mutually linked into discrete centrosymmetric dimmers by weak intermolecular hydrogen bond of the N−H···N type formed between NH group and thiazole nitrogen atom (N2−H2N···N1^i; $i = x, y, {}^3/_2 - z$; N2−H2N, 0.84(3) Å; H2N···N1, 2.16(2) Å; N2···N1, 3.002(2) Å; ∠N2−H2N···N1, 178(1)°) (Figure 2b). No other types of hydrogen bonds are found.

In our previous work we reported molecular and crystal structures of compounds 2-chloro-*N*-(6-cyanobenzothiazol-2-yl)benzamide **4** and 4-cyano-*N*-(benzothiazol-2-yl)benzamide **6**.[14,30] Both compounds also show similar crystal packing pattern of mutually linked molecules into discrete centrosymmetric dimers by weak intermolecular hydrogen bond of the N−H···N type. They are formed between the amide group and N atom of benzothiazole moiety, while in compound **15** (present work) they are formed between the amino group and N atom of benzothiazole moiety.

Therefore, we assume that analogous compounds could also form H-bonds not just in crystals but also in aqueous biological media. Since H-bonding is an important way of interaction of biologicaly active molecules with a potential target, it could be suggested that the ability of prepared molecules to form H-bonds in aqueous biological media may play a role in their biological activity.

Biological Results and Discussion

Antiproliferative Activity. The compounds **7**−**31** were tested for their potential antiproliferative effect on a panel of human cell lines, six of which were derived from cancer cell types: HeLa (cervical carcinoma), Hep-2 (laryngeal carcinoma), MCF-7 (breast carcinoma), SW 620 (colon carcinoma), MiaPaCa-2 (pancreatic carcinoma), H 460 (lung carcinoma), and WI 38 (diploid fibroblasts). The results are expressed as IC_{50} (μM) summarized in Tables 1 and 2. The cyano substituted benzothiazoles (**11**−**17**) were poorly soluble in aqueous cell culture medium; therefore, the highest concentration tested was 10^{-5} M, yet the precipitation still occurred during the test period (72 h). Nevertheless, all compounds except **11** showed antiproliferative activity at least toward some cell types (e.g., MiaPaCa-2), whereby 6-cyano-2-(*N*-(pyrimidin-2-yl)amino)benzothiazole **17** was the most active compound (Table 1). Cyano-substituted benzothiazol-2-ylbenzamides **3**−**6** and amidino derivatives **25** and **27** were not tested for their antiproliferative effect because of their poor solubility in aqueous cell culture medium.

These results (Table 1) point out that (i) two cyano groups (**11**) strongly reduce the activity, (ii) replacing a pyridine with the pyrimidine ring without any substituent significantly increases the antiproliferative activity, (iii) the position of methyl group at the pyridine ring (R2) does not significantly alter the activity.

On the other hand, all isopropylamidino- and imidazolinyl-substituted benzothiazoles showed a strong antiproliferative effect on the tested cell line panel (Table 2 and Figure 3), while isopropylamidino-substituted benzothiazol-2-ylbenzamides **7**−**10** showed modest and mostly similar effects in all cell lines tested.

Still, the imidazolinyl-substituted derivatives **26**−**31** show more prominent, mostly nonselective cytotoxic activity, while the isopropylamidino analogues **18**−**24** have more differential activity showing less inhibitory effect in normal cells. Considering the isopropylamidino-substituted analogues, it was noticed that the position of methyl group influences their antiproliferative activity, whereby the C-5 position diminishes the activity. Moreover, all isopropylamidino-substituted compounds showed significant selectivity; they strongly inhibited the growth of tumor compared with normal cells. In contrast, all imidazolinyl-substituted benzothiazoles showed almost identical activity. In order to shed more light on the mechanism of action of these compounds, we tested the most interesting (active) and selective isopropyl derivatives **21** and **22** and their direct imidazolinyl analogues **28** and **29** for their effects on the cell cycle of the most sensitive tumor cell line H 460, along with their potentials to induce apoptosis in these cells.

Cell Cycle Perturbations. The benzothiazole compounds at various concentrations result in a number of distinct perturbations in cell cycle progression of H 460 cells (Figure 4), confirming that the previously discussed structural differences have strong impact on the activity. For example, isopropylamidino derivative **21**, being less active by an order of magnitude than other compounds, also showed notable effects on the cell cycle only at significantly higher concentration than other compounds (50 μM, which is 5 times higher than its IC_{50}), whereby it induced both G1 and G2 delay, along with the

Scheme 1. Synthesis of Isopropylamidino-Substituted Benzothiazol-2-ylbenzamides **7**−**10**

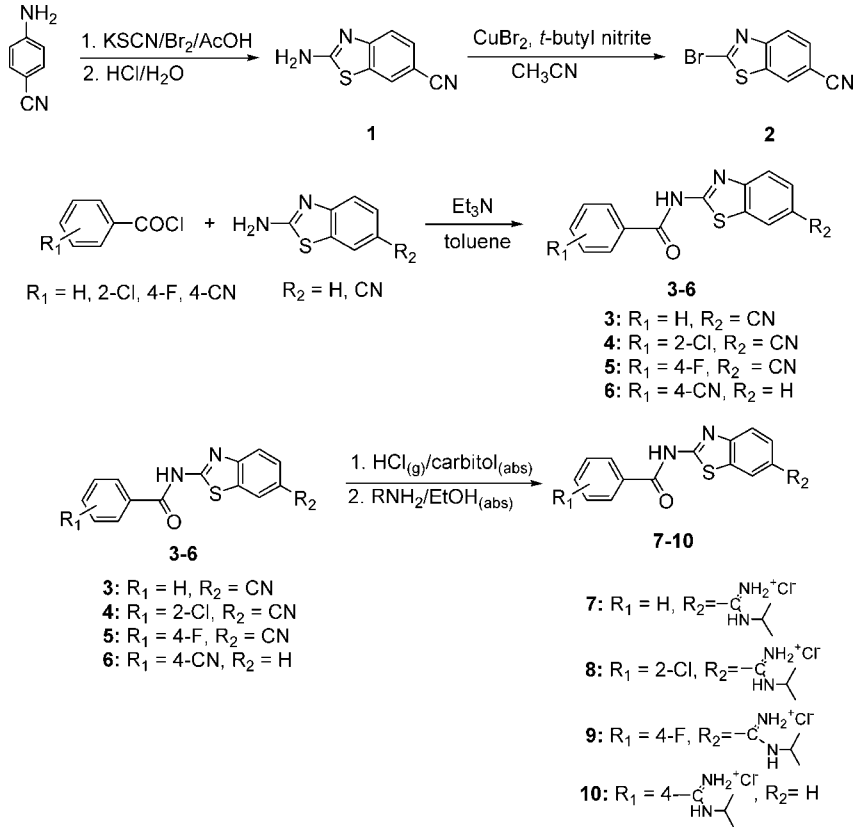

Scheme 2. Synthesis of Cyano- and Amidino-Substituted 2-(Hetero)arylaminobenzothiazoles **11**−**31**

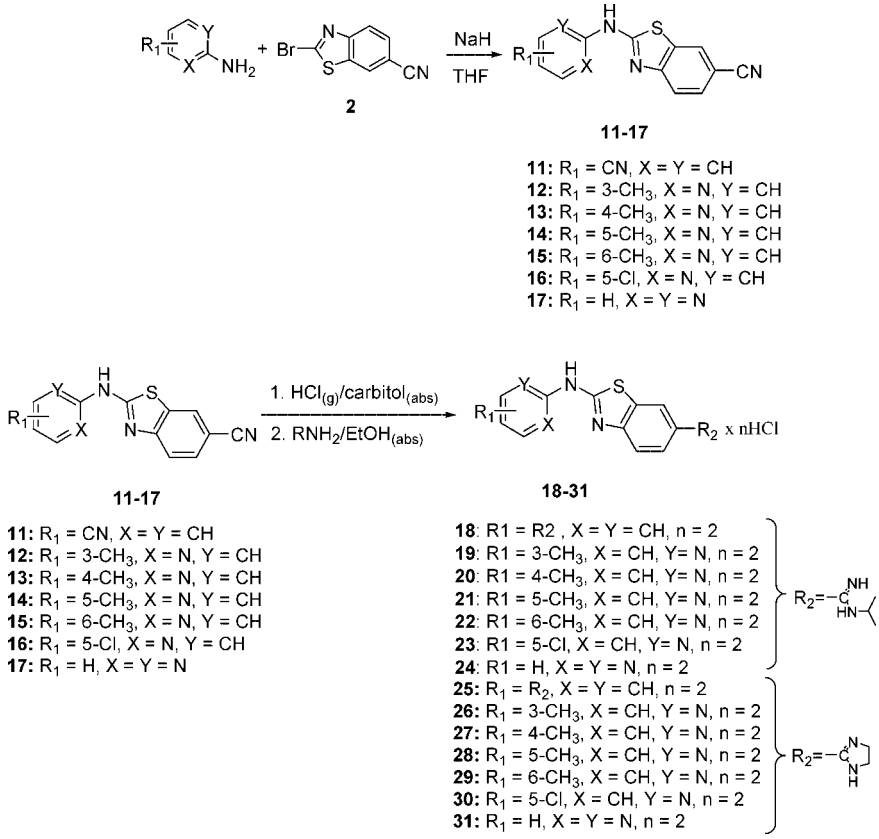

reduction of the percentage of cells in S-phase (Figure 4A,B). Similarly, its imidazolinyl analogue **28** showed minor changes at both time points.

On the other hand, both analogues bearing a methyl group at position 6 of the pyridine ring (**22** and **29**) showed very interesting and drastic cell cycle perturbations, whereby lower

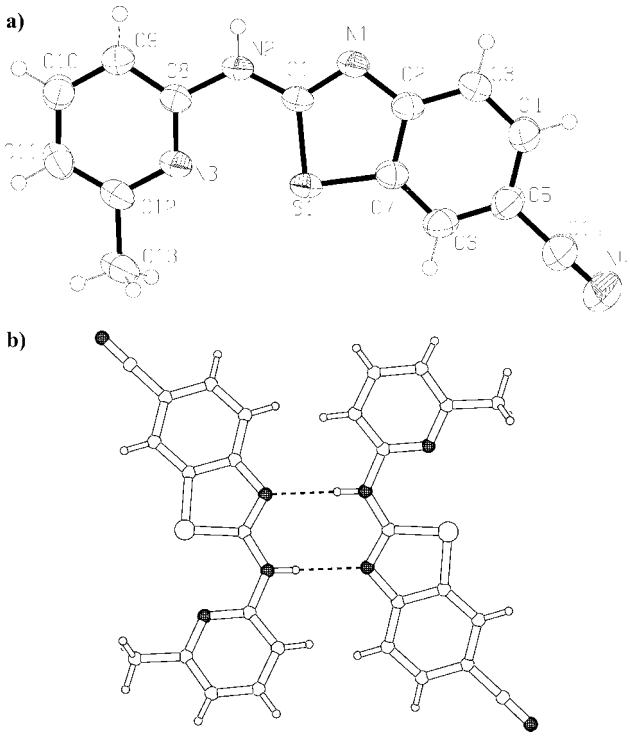

Figure 2. (a) ORTEP-3 (version 1.08) drawing of the molecular structure of 6-cyano-2-(*N*-(6-methylpyridin-2-yl)amino)benzothiazole **15** with the atomic numbering scheme. The thermal ellipsoids are drawn at the 50% probability level at 293 K. (b) Crystal structure of 6-cyano-2-(*N*-(6-methylpyridin-2-yl)amino)benzothiazole **15** viewed along the *y* axis. Hydrogen bonds of the N−H···N type are shown as dashed lines.

concentrations lead to an increase in the percentage of cells in the G1 phase. In contrast, 10 μM of both compounds did not lead to a similar G1 increase but rather resulted in a marked increase in the percentage of cells in G2/M. All concentrations of tested compounds reduced the percentage of cells in the S-phase. In addition, **22** and **29** increased the percentage of cells in sub-G1, pointing to the induction of apoptosis. Moreover, compound **22** at 50 μM induced apoptosis in about 40% of cells after 24 h, while all cells died after 48 h of treatment (data not shown).

Annexin V Assay. To confirm the previously obtained results, we assessed the annexin V assay, as a more sensitive method for apoptosis detection and for quantification after 48 h of treatment with compounds **21**, **22**, **28**, and **29** at the same concentrations as in the cell cycle perturbations assay. Indeed, we confirmed that all compounds induced apoptosis in a dose-dependent manner, whereby the effect of compounds **22** and **29** was the most prominent (Figure 5 and data not shown).

Our results demonstrate that different concentrations of amidinobenzothiazoles **22** and **29** lead to distinct cellular responses. These responses could be correlated with (i) specific cellular localization patterns or (ii) different kinetics of inhibition of specific cell-cycle-related protein. We propose that low concentrations of compounds might selectively accumulate in cell membrane and/or cytoplasm, resulting in a G1 checkpoint activation and consequently arrest cell proliferation. Higher concentrations of compounds accumulate in the cytoplasm and nucleus where they directly interfere with DNA synthesis, activate a G2 checkpoint, and consequently block cell cycle prior to entry into M-phase. High concentrations resulted in sufficient damage to trigger apoptosis. Similar results were described by Serafim et al. who showed that plant isoquinoline alkaloid berberine induced different cell cycle responses at different concentrations and time points.[31]

QSAR Analysis

A series of potentially relevant physical descriptors were calculated using the program Volsurf.[32] Principal components (PC) analysis was accomplished in order to determine distribution of the compounds in the *X*-variable space, i.e., space of physicochemical descriptors. Distribution of the compounds in the descriptor space is shown in the score plot of the first two principal components (Figure 6).

Most of the cyano-substituted compounds are grouped on the left side of the plot. The exception is compound **17**, pointing to its significantly better solubility that correlates perfectly with our experimental results, since as discussed previously, **17** was the most active compound among cyano-substituted compounds, which were in general poorly soluble. Such distribution is mostly determined by the WO1 variable values, representing the volume of the oxygen probe at an energy level of −0.837 kJ/mol (which predominantly describes PC1 and which is for the cyano-substituted compounds grouped on the left side of the graph about 20% lower than for the other compounds), and WN1 variable values, representing the volume of amide molecule probe at an energy level of −0.837 kJ/mol (which predominantly describes PC2). These two descriptors describe most of the variability in the *X*-variables space, i.e., space of the calculated descriptors (Figure 7). Compound **31** is the only non-cyano-substituted compound situated at the left half of the score plot. Among properly soluble compounds it is the smallest one (i.e., it has the smallest V and S) with very high WN1 value (only compound **9** has higher WN1 value). Although it has the smallest WO1 in the group (about 370), this value is much above WO1 values determined for cyano-substituted compounds (WO1 < 100).

In general, the oxygen and amide probe volumes are proportional to compound hydrophilicity, while their shapes correlate with the ability of the compound to fit into putative receptor's or transporter's active site. Compounds with small WO1 are grouped on the left side of the score plot, and those with small WN1 are at its lower part. Compounds with small WO1 are poorly soluble, and as a consequence, their activity could not be precisely determined.

Further, we correlated the experimental results (IC_{50} for growth inhibition) with the physical and chemical properties of the compounds using partial least-squares (PLS) analysis. For these calculations we used two data sets: (A) all compounds that do not contain the cyano substitutent; (B) all compounds on the right side of the score plot. Both groups contain 16 compounds, and they differ in one compound only; the first group contains compound **17**, and the second one contains compound **31**. The statistical parameters of the obtained PLS models are given in Table 3. The models with the highest predictive performances are derived for HeLa, Mia PaCa-2, and SW 620 cell lines (see also Figure 8).

The optimal dimensionality depends on the cell line considered, but it is never above 3. The goodness of the model was defined by fitting (R^2 and standard deviation of the error of calculation, SDEC) and cross-validation (Q^2 and SDEP) parameters (see Table 3 for the definitions of these parameters).

From the obtained models we could elucidate which physicochemical descriptors of the compounds, i.e., *X*-variables, are most relevant for growth inhibition of different cell lines. Variables with the highest absolute weights (either large positive or negative values) are considered to be the most significant to

Table 1. In Vitro Inhibition of the Cyano-Substituted Compounds **11**−**17** on the Growth of Tumor Cells and Normal Human Fibroblasts (WI 38)

	IC_{50} (μM)[a]					
compd	WI 38	Hep-2	HeLa	MiaPaCa-2	SW 620	MCF-7
11	>10	>10	>10	>10	>10	>10
12	2.3 ± 0.8	>10	>10	3 ± 0.2	3 ± 2	>10
13	≥10	7 ± 3	3 ± 2	4 ± 0.04	4 ± 2	>10
14	4 ± 4	>10	9 ± 1	5 ± 4	>10	>10
15	>10	>10	8 ± 2	6 ± 3	4 ± 1	8 ± 2
16	>10	>10	>10	6 ± 4	≥10	10
17	≥10	5 ± 2	5 ± 2	3 ± 2	9 ± 1	7 ± 1

[a] IC_{50}: the concentration that causes a 50% reduction of the cell growth.

Table 2. In Vitro Inhibition of the Isopropylamidino- (**7**−**10**, **18**−**24**) and Imidazolinyl- (**26**−**31**) Substituted Benzothiazole Derivatives on the Growth of Tumor Cells and Normal Human Fibroblasts (WI 38)

	IC_{50} (μM)[a]					
compd	WI 38	H 460	HeLa	MiaPaCa-2	SW 620	MCF-7
7	>100	15 ± 1	16 ± 5	38 ± 11	30 ± 0.4	22 ± 5
8	61 ± 31	59 ± 9	23 ± 8	45 ± 13	45 ± 11	16 ± 3
9	>100	22 ± 2	13 ± 1	32 ± 3	35 ± 5	13 ± 2
10	16 ± 3	16 ± 2	9 ± 7	17 ± 4	17 ± 2	13 ± 5
18	92 ± 4	16 ± 7	18 ± 2	30 ± 18	18 ± 6	6 ± 8
19	14 ± 1.6	2 ± 0.4	5 ± 1.4	3 ± 1	5 ± 3	2 ± 0.7
20	12.5 ± 0.8	2 ± 0.4	4 ± 1	3 ± 0.2	3 ± 0.9	2 ± 0.7
21	31 ± 1	15 ± 0.9	12 ± 2	14 ± 0.4	12 ± 2	8 ± 0.04
22	19 ± 1	3 ± 1	4 ± 3	3 ± 1	9 ± 1	3 ± 2
23	17 ± 0.5	15 ± 0.7	9 ± 5	12 ± 0.1	13 ± 2	5 ± 4
24	75 ± 25	5 ± 0.4	7 ± 3	11 ± 8	15 ± 3	13 ± 3
26	NT[b]	2 ± 0.2	3 ± 0.1	3 ± 1	2 ± 0.4	2 ± 0.2
28	6 ± 2	2 ± 0.4	2 ± 1	2 ± 0.02	1 ± 0.2	2 ± 1
29	2 ± 1	2 ± 0.2	2 ± 0.9	2 ± 0.3	2 ± 1	2 ± 1
30	1 ± 0.1	1.5 ± 0.2	1 ± 0.01	1.6 ± 0.2	1.3 ± 0.1	1.4 ± 0.2
31	1.7 ± 0.06	1.6 ± 0.08	1.4 ± 0.05	1.8 ± 0.1	1.7 ± 0.6	1.7 ± 0.0

[a] IC_{50}: the concentration that causes a 50% reduction of the cell growth. [b] NT: not tested.

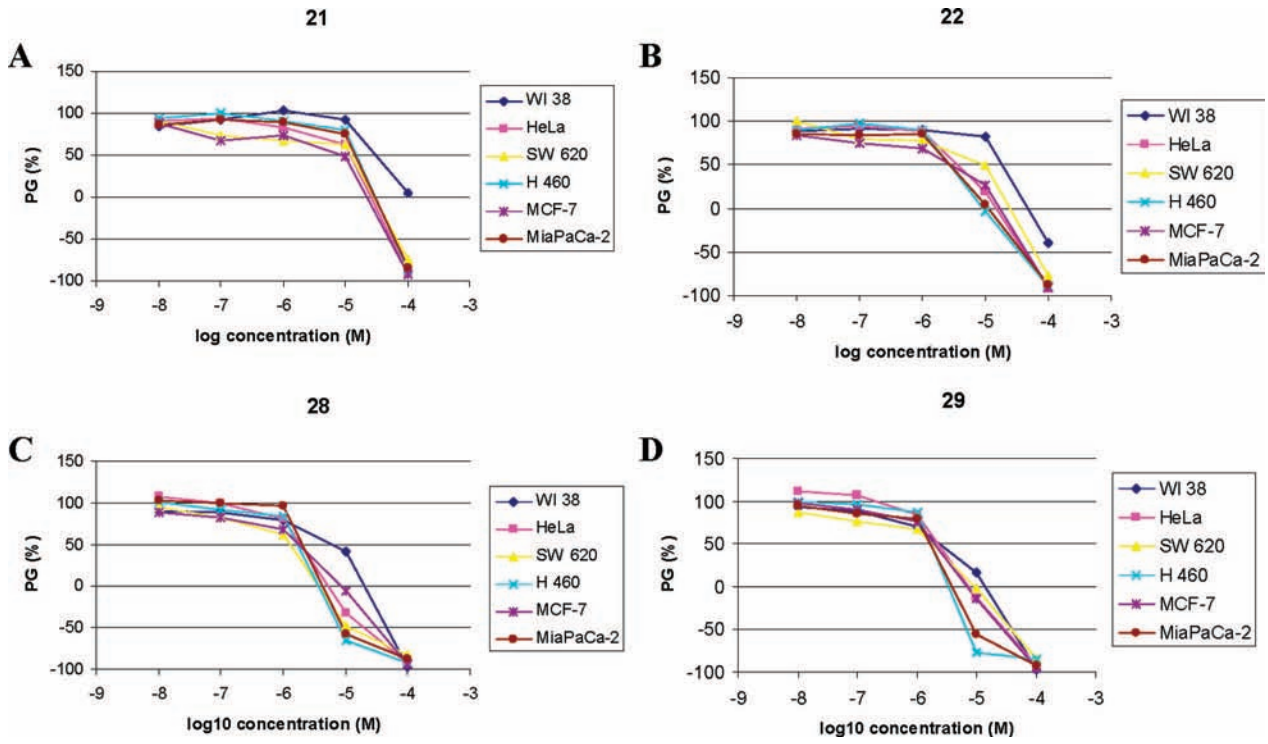

Figure 3. Dose−response profiles for compounds **21** (A), **22** (B), **28** (C), and **29** (D). PG = percentage of growth.

explain the compound efficiency on a certain cell line. The descriptors specific for a certain cell line can be found by comparing the *X*-variables with the highest weights in different models. Weights for the most relevant descriptors obtained in HeLa, MiaPaCa-2, and SW 620 models are given in Figure 9.

Overall, it could be concluded that the impact of descriptors on the inhibition of growth of these cell lines is pretty even. However, the WO descriptors are significantly more important for SW 620 than other cell lines, pointing to the importance of molecular polarizability, while molecular volume and

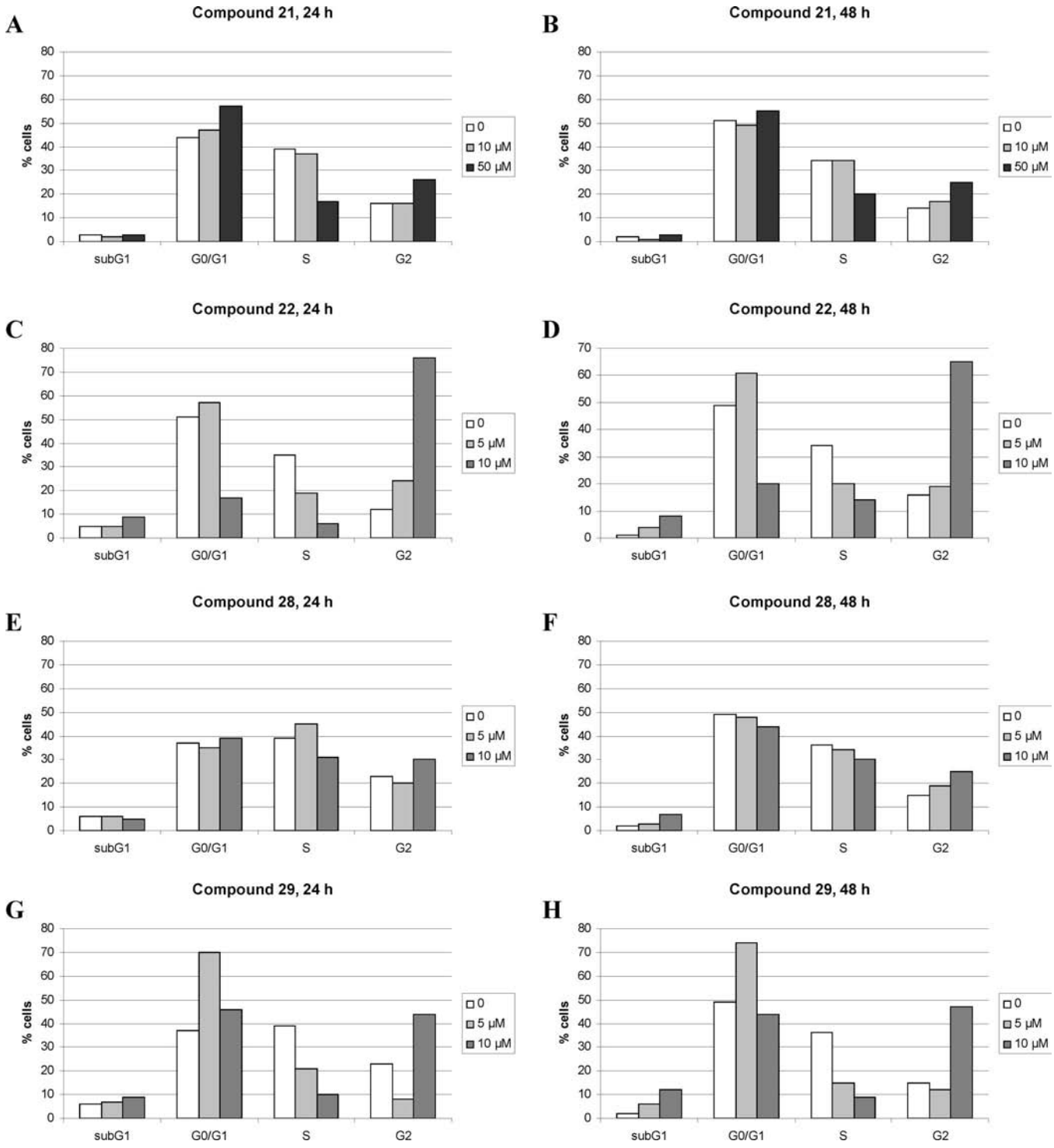

Figure 4. Cell cycle analysis of H 460 cells treated with 5, 10, and 50 μM compounds **21**, **22**, **28**, and **29** for 24 h (A, C, E, G, respectively) or 48 h (B, D, F, H, respectively). See results and discussion section for details.

surface are relatively important descriptors for MiaPaCa-2 and HeLa; i.e., benzothiazoles substituted with imidazolinyl group, the molecules with the smallest surface and volume, showed the strongest antiproliferative effect on these lines.

The QSAR model could not be derived for WI 38 cell line, while for the MCF-7 cell line it is of a rather low quality, with no predictive ability. The partial explanation lies in the nature of WI 38 cells, which proliferate slowly compared to other cell lines. Therefore, the influences of the tested compounds are quite different, making the results inadequate to obtain satisfactory models.

Conclusion

A series of novel cyano- and amidinobenzothiazole derivatives (**3**−**31**) were prepared by multistep synthesis. All isopropylamidino- and imidazolinyl-substituted benzothiazoles showed strong antiproliferative effect on the tumor cell lines, whereby imidazolinyl-substituted derivatives (**25**−**31**) showed more

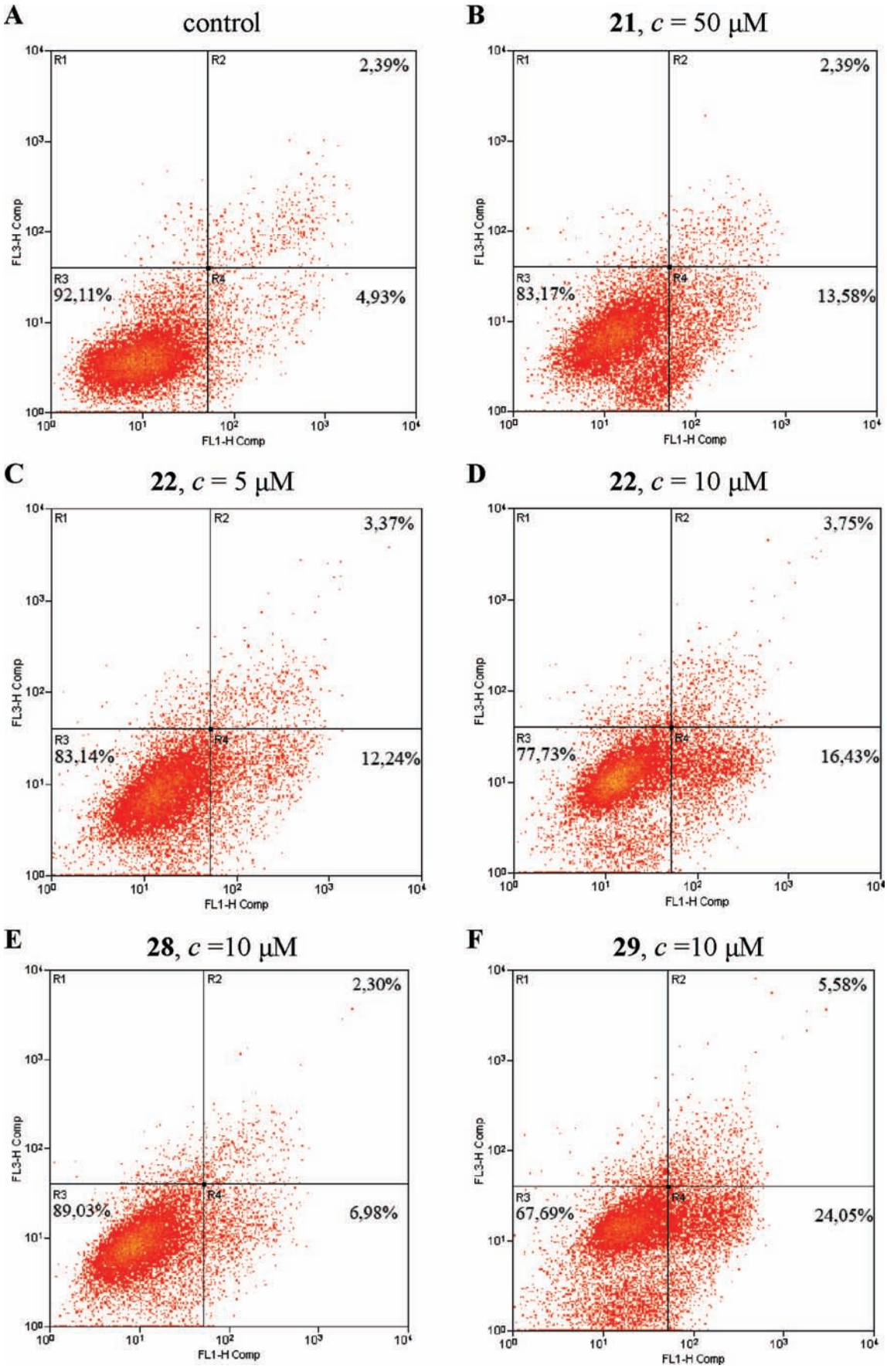

Figure 5. Annexin-V assay on H 460 cells treated with compounds **21** ($c = 50\ \mu$M) (B), **22** ($c = 5\ \mu$M (C) and $c = 10\ \mu$M (D)), **28** ($c = 10\ \mu$M) (E), **29** ($c = 10\ \mu$M) (F) for 48 h. Control, vehicle-treated cells are shown in (A). The figure shows representative dot-plots of annexin V Alexa Fluor 488 (*x*-axis)/7-AAD (*y*-axis) fluorescence. The percentages of population undergoing early and late apoptotic events are indicated in the lower (R4) and upper (R2) right quadrant, respectively. Lower left quadrant (R3) represents the viable cells.

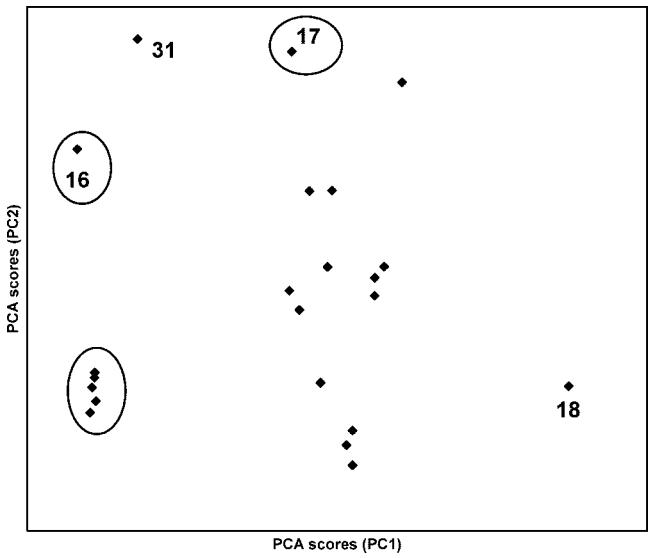

Figure 6. Score plot of the first (PC1) and second (PC2) principal components of the physicochemical descriptors (determined by the program Volsurf, see Experimental Section) for 23 compounds. These two principal components describe about 81% of variance among the *X*-variables. Cyano-substituted compounds are encircled.

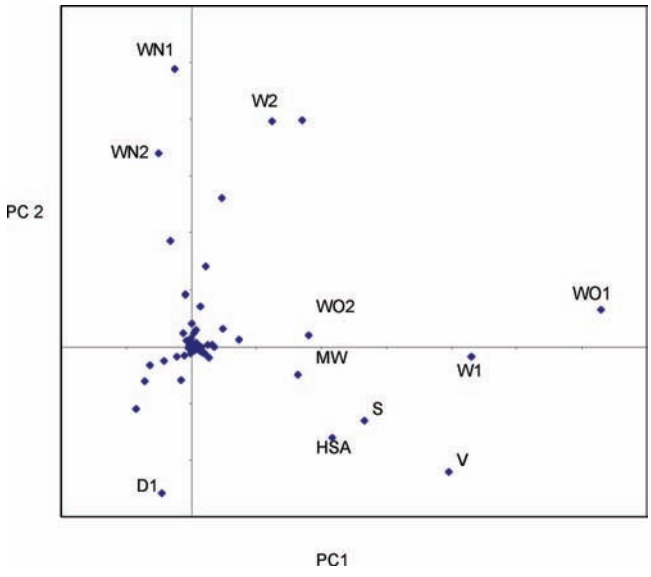

Figure 7. Loading plot of the first (PC1) and second (PC2) principal components of the physicochemical descriptors (determined by the program Volsurf) for 23 compounds. Descriptors that are the most important for differentiation of compounds are indicated. Their meaning is the following: WO1 and WO2; W1 and W2; W1N and W2N are the volumes of the oxygen probe, water molecule, and amide molecule, respectively. Interaction fields are at two different energy levels: −0.837 and −1.674 kJ/mol. D1 describes the volume of the hydrophobic region (interaction with the DRY probe); V represents molecular volume; S describes molecular surface; HAS is the hydrophobic surface area.

prominent, mostly nonselective cytotoxic activity, while the isopropylamidino analogues (**18**−**24**) had more differential activity showing less inhibitory effect on normal cells. The position of methyl group in pyridine ring of both amidino-substituted groups of derivatives played a role in their antiproliferative activity, whereby the C-5 position diminished the activity while its C-6 position led to very interesting and drastic cell cycle perturbations. Lower concentrations of **22** and **29** (5 μM) led to an increase in the percentage of cells in G1, while higher concentrations (10 μM) of both compounds resulted in a marked increase of cells in G2/M phase, while all concentrations of tested compounds reduced the S-phase. In addition, **22** and **29** increased the percentage of cells in sub-G1, pointing to the induction of apoptosis.

The principal components analysis and QSAR modeling revealed that the cyano-substituted compounds **11**−**17** were highly hydrophobic and consequently poorly soluble. The exception was compound **17**, thus correlating with its higher biological activity. The best models were derived for the HeLa cell line. The molecules with the smallest surface and volume showed the strongest antiproliferative effect on this line.

Experimental Section

Chemistry. Melting points were determined on a Kofler hot stage microscope and are uncorrected. IR spectra were recorded on a Nicolet Magna 760 spectrophotometer in KBr disks. ^{1}H and ^{13}C NMR spectra were recorded on either a Varian Gemini 300 or a Bruker Avance DPX 300 spectrometer using TMS as an internal standard in DMSO-d_6. Elemental analysis for carbon, hydrogen, and nitrogen were performed on a Perkin-Elmer 2400 elemental analyzer. Where analyses are indicated only as symbols of elements, analytical results obtained are within ±0.4% of the theoretical value. All compounds were routinely checked by TLC with Merck silica gel 60F-254 glass plates. Experimental and spectroscopic data for cyano derivatives **1**−**6** and **11**−**17** with the reference list are in Supporting Information.

General Method for the Synthesis of Amidino Substituted Benzothiazoles (7−10, 18−31). Amidino-substituted benzothiazoles (**7**−**10**, **18**−**31**) were prepared by modified Pinner reaction.[27] The suspension of the corresponding cyano-substituted amides (0.4 g) or cyano-substituted 2-(hetero)arylaminobenzothiazoles (0.2 g) in absolute carbitole (5 or 7 mL) at 0 °C was saturated with dry HCl gas. After the mixture returned to room temperature, the flask was stoppered and the contents were stirred until IR spectra indicated the lack of the cyano peak (3 days). The corresponding imido ester hydrochloride intermediate (90−95% yield) was precipitated from the solution by the addition of dry diethyl ether, filtered off, washed with dry ether, and dried under reduced pressure over KOH.

Isopropylamidines. Isopropylamine (3 equiv) was added to a suspension of the corresponding imido ester hydrochloride and absolute ethanol (5 mL) under a nitrogen atmosphere. The reaction mixture was left to stir for 24 h at room temperature. After 24 h diethyl ether was added to the reaction mixture and the precipitate was filtered off and dried. The crude product was dissolved in absolute ethanol (5 mL) at 0 °C and saturated with dry HCl gas. The corresponding isopropylamidine salt was precipitated from the solution by addition of dry diethyl ether, filtered off, washed with dry ether, and dried under reduced pressure over KOH.

Imidazolinylamidines. Ethylendiamine (3 equiv) was added to a suspension of the corresponding imido ester hydrochloride and absolute ethanol (5 mL) under a nitrogen atmosphere and left to reflux for 4 h. After 4 h the reaction mixture was left to stir at room temperature for the next 12 h. After 12 h, diethyl ether (20−40 mL) was added to the reaction mixture and the precipitate was filtered off and dried. The crude product was recrystallized from water (3−5 mL) to remove the remaining diethylamine hydrochloride salt, filtered off, and dried. Dry product was dissolved in absolute ethanol (5 mL), and the suspension was saturated with dry HCl gas at 0 °C. The corresponding imidazolinylamidine salt was precipitated from the solution by the addition of dry diethyl ether, filtered off, washed with dry ether, and dried under reduced pressure over KOH.

***N*-(6-(*N*-Isopropyl)amidinobenzothiazol-2-yl)benzamide Hydrochloride (7).** White powder was isolated (0.184 g, 52.8%), mp = 296−298 °C. IR (KBr) (ν_{max}/cm^{-1}): 3417, 1682 (C═O), 1604 (C═N). ^{1}H NMR (DMSO) (δ/ppm): 12.93 (brs, 1H, NH), 9.70 (d, 1H, J = 7.83 Hz, $H_{amidine}$), 9.56 (s, 1H, $H_{amidine}$), 9.29 (s, 1H, $H_{amidine}$),

Table 3. Predictive Performances of the Best Volsurf Models Derived for Two Data Sets (A, Top, and B, Bottom, Both Containing 16 Compounds (for Description, See Text)) Acting on Different Cell Line Types

model	cell line	LV[a]	Q^{2b}	R^{2c}	SDEP[d]	SDEC[e]
A	HeLa	1	0.58	0.69	4.2	3.6
	MiaPaCa-2	2	0.59	0.78	8.9	6.6
	SW 620	3	0.58	0.76	8.3	6.2
	MCF-7	2	0.33	0.56	5.1	4.1
B	HeLa	1	0.56	0.68	4.2	3.6
	MiaPaCa-2	1	0.63	0.77	8.6	6.8
	SW 620	2	0.54	0.73	8.7	6.6
	MCF-7	3	0.31	0.52	5.2	8.8

[a] LV is the number of latent variables. [b] Q^2 is the cross-validated predictive performance and is given by $Q^2 = 1 - (\sum_{i=1}^{n} (y_{\exp(i)} - y_{\mathrm{pred}(i)})^2)/(\sum_{i=1}^{n} (y_{\exp(i)} - \langle y_{\exp} \rangle)^2)$, where y_{pred} corresponds to the value of IC_{50} predicted with the model for compound i, $y_{\exp}$ is the experimentally determined inhibition, IC_{50}, of the compound. [c] R^2 is the equivalent of Q^2 calculated for fitting. [d] SDEP is the standard deviation in cross-validated prediction and is given by $\mathrm{SDEP} = [(\sum_{i=1}^{n} (y_{\exp(i)} - y_{\mathrm{pred}(i)})^2)/(n)]^{1/2}$. [e] SDEC is the equivalent of SDEP for fitting.

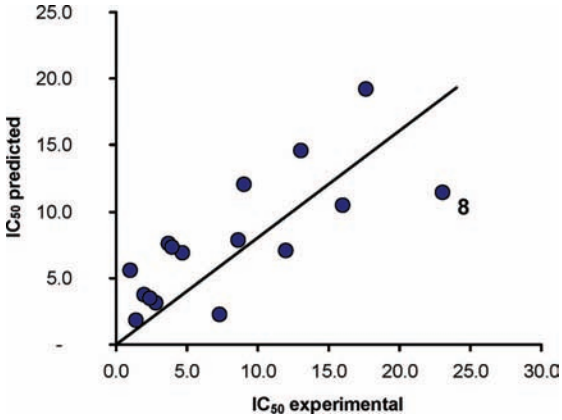

Figure 8. Plot of experimental (*X*-axis) versus predicted (*y*-axis) growth inhibition (IC_{50}) for HeLa cell line with the outlier indicated (the compound for which the discrepancy between the predicted and experimental activity is larger than 2 times the standard deviation).

8.50 (d, 1H, J = 1.6 Hz), 8.16 (d, 2H, J = 7.41 Hz), 7.94 (d, 1H, J = 8.47 Hz), 7.82 (dd, 1H, J_1 = 8.47 Hz, J_2 = 1.6 Hz), 7.71−7.56 (m, 3H), 4.24−4.11 (m, 1H, CH), 1.30 (d, 6H, J = 6.3 Hz, CH_3). ^{13}C NMR (DMSO) (δ/ppm): 166.90, 162.53, 162.05, 152.11, 148.40, 133.65, 132.03, 129.19, 128.93, 126.89, 124.66, 123.36, 120.65, 45.62, 21.78. MS *m*/*z*: 339 (M^+ − Cl, 100%). Anal. ($C_{18}H_{19}ClN_4OS$) C, H, N.

2-Chloro-*N*-(6-(*N*-isopropyl)amidinobenzotiazol-2-yl)benzamide Hydrochloride (8). White powder was isolated (0.182 g, 69.9%), mp = 291−292 °C. IR (KBr) (ν_{max}/cm^{-1}): 3414, 3053, 1674 (C═O), 1622 (C═N). ^{1}H NMR (DMSO) (δ/ppm): 13.27 (s, 1H, NH), 9.68 (d, 1H, J = 7.11 Hz, $H_{amidine}$), 9.53 (s, 1H, $H_{amidine}$), 9.20 (s, 1H, $H_{amidine}$), 8.51 (s, 1H), 7.97 (d, 1H, J = 8.46 Hz), 7.80 (d, 1H, J = 8.31 Hz), 7.73 (d, 1H, J = 7.56 Hz), 7.64−7.48 (m, 3H), 4.18−4.07 (m, 1H, CH), 1.30 (d, 6H, J = 6.12 Hz, CH_3). ^{13}C NMR (DMSO) (δ/ppm): 166.52, 162.13, 161.38, 152.28, 134.21, 132.88, 132.13, 130.78, 130.41, 130.11, 127.84, 126.92, 124.89, 123.40, 121.15, 121.13, 45.59, 21.75. Anal. ($C_{18}H_{18}Cl_2N_4OS$) C, H, N.

4-Fluoro-*N*-(6-(*N*-isopropyl)amidinobenzotiazol-2-yl)benzamid Hydrochloride (9). White powder was isolated (0.137 g, 52.0%), mp = 296 − 298 °C. IR (KBr) (ν_{max}/cm^{-1}): 3428, 3052, 1675 (C═O), 1604 (C═N). ^{1}H NMR (DMSO) (δ/ppm): 13.21 (brs, 1H, NH), 9.66 (d, 1H, J = 7.5 Hz, $H_{amidine}$), 9.54 (s, 1H, $H_{amidine}$), 9.24 (s, 1H, $H_{amidine}$), 8.49 (s, 1H), 8.27−8.22 (m, 2H), 7.95 (d, 1H, J_1 = 8.46 Hz), 7.81 (dd, 1H, J_1 = 8.49 Hz, J_2 = 1.29 Hz), 7.46−7.40 (m, 2H), 4.17−4.08 (m, 1H, CH), 1.31 (d, 6H, J = 6.3 Hz, CH_3). ^{13}C NMR (DMSO) (δ/ppm): 165.79, 165.53, 164.66, 164.13, 162.97, 131.98, 131.39, 128.16, 126.50, 123.17, 120.61, 116.90, 115.69, 45.64, 21.79. Anal. ($C_{18}H_{18}ClFN_4OS$) C, H, N.

4-(*N*-Isopropylamidino)-*N*-(benzothiazol-2-yl)benzamide Hydrochloride (10). 10 was prepared by the above-described procedure to give physical constants in accordance with literature values, yield 41.9%, mp = 288−289 °C (lit.[14] mp = 288−289 °C). The ^{1}H and ^{13}C NMR spectra are in accordance with literature data.

6-(*N*-Isopropylamidino)-2-(*N*-(4-((*N*-isopropylamidino)phenyl))amino)benzothiazole Dihydrochloride (18). Beige powder was isolated (0.11 g, 32.5%), mp = 294−295 °C. IR (KBr) (ν_{max}/cm^{-1}): 3413, 3225, 1667, 1614. ^{1}H NMR (DMSO) (δ/ppm): 12.10 (brs, 1H, NH), 9.60 (d, 1H, J = 8.25 Hz, $H_{amidine}$), 9.53 (d, 1H, J = 8.07 Hz, $H_{amidine}$), 9.46 (s, 1H, $H_{amidine}$), 9.42 (s, 1H, $H_{amidine}$), 9.15 (s, 1H, $H_{amidine}$), 9.07 (s, 1H, $H_{amidine}$), 8.31 (d, 1H, J = 1.37 Hz), 8.09 (d, 2H, J = 8.67 Hz), 7.82 (d, 3H, J = 8.4 Hz), 7.71 (dd, 1H, J_1 = 8.37 Hz, J_2 = 1.32 Hz), 4.17−4.07 (m, 2H, CH), 1.29 (d, 12H, J = 6.3 Hz, CH_3). ^{13}C NMR (DMSO) (δ/ppm): 163.99, 161.55, 161.06, 155.11, 144.33, 130.63, 129.58, 126.33, 123.04, 122.05, 121.98, 119.13, 117.40, 45.03, 44.93, 21.29, 21.27. Anal. ($C_{21}H_{28}Cl_2N_6S$) C, H, N.

6-(*N*-Isopropyl)amidino-2-(*N*-(3-methylpyridin-2-yl)amino)benzothiazole Dihydrochloride (19). Beige powder was isolated (0.2 g, 66.8%), mp = 210−212 °C. IR (KBr) (ν_{max}/cm^{-1}): 3406, 3085, 1667, 1627. ^{1}H NMR (DMSO) (δ/ppm): 9.60 (d, 1H, J = 7.89 Hz, $H_{amidine}$), 9.47 (d, 1H, J = 7.89 Hz, $H_{amidine}$), 9.14 (s, 1H, $H_{amidine}$), 8.36 (s, 1H), 8.30 (d, 1H, J = 4.35 Hz), 7.80−7.72 (m, 3H), 7.09 (dd, 1H, J_1 = 6.80 Hz, J_2 = 5.44 Hz), 5.05 (brs, 2H, NH_2^+), 4.18−4.09 (m, 1H, CH), 2.41 (s, 3H, CH_3), 1.29 (d, 6H, J = 6.27 Hz, CH_3). ^{13}C NMR (DMSO) (δ/ppm): 163.37, 162.22, 152.32, 149.81, 143.09, 140.45, 131.95, 126.70, 123.14, 122.71, 121.79, 118.74, 118.50, 45.52, 21.80, 17.35. Anal. ($C_{17}H_{21}Cl_2N_5S$) C, H, N.

6-(*N*-Isopropyl)amidino-2-(*N*-(4-methylpyridin-2-yl)amino)benzothiazole Dihydrochloride (20). Beige powder was isolated (0.15 g, 79.1%), mp = 238−240 °C. IR (KBr) (ν_{max}/cm^{-1}): 3411, 3066, 1649, 1586. ^{1}H NMR (DMSO) (δ/ppm): 9.56 (d, 1H, J = 7.95 Hz, $H_{amidine}$), 9.42 (s, 1H, $H_{amidine}$), 9.07 (s, 1H, $H_{amidine}$), 8.34 (s, 1H), 8.27 (d, 1H, J = 5.16 Hz), 7.77 (d, 1H, J = 8.4 Hz), 7.71 (d, 1H, J = 8.4 Hz), 7.07 (s, 1H), 6.96 (d, 1H, J = 5.1 Hz), 4.56 (brs, 2H, NH_2^+), 4.15−4.04 (m, 1H, CH), 2.35 (s, 3H, CH_3), 1.29 (d, 6H, J = 6.24 Hz, CH_3). ^{13}C NMR (DMSO) (δ/ppm): 163.05, 162.30, 153.42, 151.44, 150.45, 146.09, 132.28, 126.57, 122.86, 122.56, 119.51, 119.18, 112.20, 45.49, 21.78, 21.28. Anal. ($C_{17}H_{21}Cl_2N_5S$) C, H, N.

6-(*N*-Isopropyl)amidino-2-(*N*-(5-methylpyridin-2-yl)amino)benzothiazole Dihydrochloride (21). White powder was isolated (0.28 g, 92.8%), mp = 246−248 °C. IR (KBr) (ν_{max}/cm^{-1}): 3439, 3055, 1668, 1650. ^{1}H NMR (DMSO) (δ/ppm): 9.61 (d, 1H, J = 8.04 Hz, $H_{amidine}$), 9.48 (s, 1H, $H_{amidine}$), 9.19 (s, 1H, $H_{amidine}$), 8.37 (s, 1H), 8.25 (s, 1H), 7.78−7.71 (m, 3H), 7.26 (d, 1H, J = 8.43 Hz), 5.60 (brs, 2H, NH_2^+), 4.20−4.09 (m, 1H, CH), 2.28 (s, 3H, CH_3), 1.29 (d, 6H, J = 6.36 Hz, CH_3). ^{13}C NMR (DMSO) (δ/ppm): 162.94, 162.10, 153.11, 149.17, 145.27, 140.69, 131.90, 127.29, 126.71, 122.87, 122.72, 118.99, 112.23, 45.53, 21.81, 17.70. Anal. ($C_{17}H_{21}Cl_2N_5S$) C, H, N.

6-(*N*-Isopropyl)amidino-2-(*N*-(6-methylpyridin-2-yl)amino)benzothiazole Dihydrochloride (22). White powder was isolated (0.24 g, 87.1%), mp > 300 °C. IR (KBr) (ν_{max}/cm^{-1}): 3413, 3052, 1668, 1620. ^{1}H NMR (DMSO) (δ/ppm): 9.48 (d, 1H, J = 7.92 Hz,

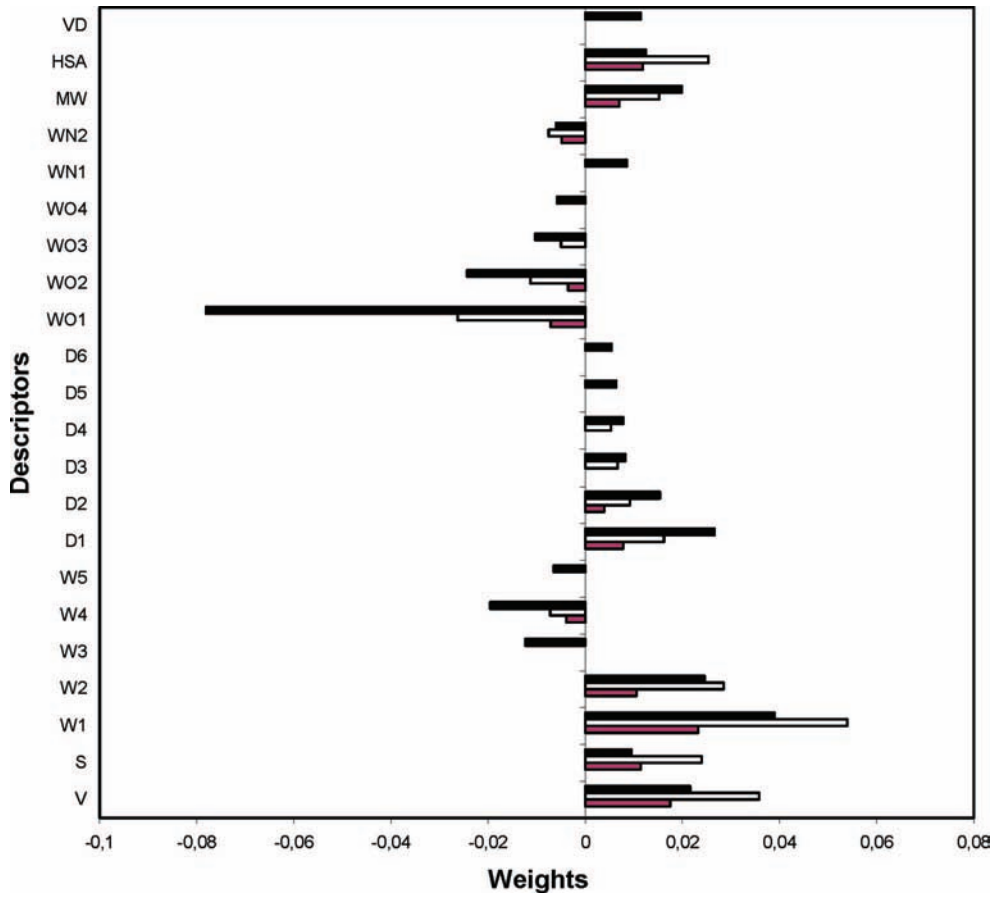

Figure 9. Most important physicochemical descriptors in models: SW 620, black; MiaPaCa-2, white; HeLa, red. Explanation of descriptors are as follows: V, volume; S, surface; W1−W6, molecular envelopes accessible by solvent water molecules: W1−W4, account for dispersion interaction and polarizability, while higher W (W5 and higher), account for polar and hydrogen bond donor−acceptor regions; D1−D6, hydrophobic regions indicating interactions with the hydrophobic probe at six different energy levels (−0.2, −0.4, −0.6, −0.8, −1.0, −1.2) × 4.186 kJ/mol; WO1−WO4, volumes of oxygen interaction fields at four different energy levels (−0.2, −0.4, −0.6, −0.8) × 4.186 kJ/mol; WN1 and WN2, volume of nitrogen interaction fields at two different energy levels (−0.2, −0.4) × 4.186 kJ/mol; MW, molecular weight; HAS, hydrophobic surface area; VD, a measure of relative partition of compounds between plasma and tissue.

$H_{amidine}$), 9.37 (s, 1H, $H_{amidine}$), 9.07 (s, 1H, $H_{amidine}$), 8.29 (s, 1H), 7.69−7.61 (m, 3H), 6.99 (d, 1H, J = 8.04 Hz), 6.87 (d, 1H, J = 7.32 Hz), 4.84 (brs, 2H, $N\underline{H}_2^+$), 4.09−4.04 (m, 1H, C$\underline{H}$), 2.46 (s, 3H, $C\underline{H}_3$), 1.22 (d, 6H, J = 6.36 Hz, $C\underline{H}_3$). ^{13}C NMR (DMSO) (δ/ppm): 162.44, 161.62, 155.17, 152.71, 150.23, 138.99, 131.74, 126.06, 122.16, 122.11, 118.49, 116.71, 108.53, 45.03, 23.15, 21.31. Anal. ($C_{17}H_{21}Cl_2N_5S$) C, H, N.

6-(*N*-Isopropyl)amidino-2-(*N*-(5-chloropyridin-2-yl)amino)benzothiazole Dihydrochloride (23). Beige powder was isolated (0.191 g, 65.4%), mp = 220−223 °C. IR (KBr) (ν_{max}/cm^{-1}): 3412, 3060, 1675, 1617). ^{1}H NMR (DMSO) (δ/ppm): 9.6 (d, 1H, J = 7.98 Hz, $H_{amidine}$), 9.47 (s, 1H, $H_{amidine}$), 9.15 (s, 1H, $H_{amidine}$), 8.45 (d, 1H, J = 2.22 Hz), 8.38 (s, 1H), 7.93 (dd, 1H, J_1 = 8.84 Hz, J_2 = 2.44 Hz), 7.77 (d, 1H, J = 8.61 Hz), 7.72 (d, 1H, J = 8.61 Hz), 7.34 (d, 1H, J = 8.84 Hz), 4.97(brs, 2H, $N\underline{H}_2^+$), 4.18−4.07 (m, 1H, C$\underline{H}$), 1.29 (d, 6H, J = 6.27 Hz, $C\underline{H}_3$). ^{13}C NMR (DMSO) (δ/ppm): 162.13, 161.67, 152.83, 149.93, 144.71, 138.40, 131.63, 126.16, 123.65, 122.48, 122.19, 118.80, 113.15, 45.03, 21.29. Anal. ($C_{16}H_{18}Cl_3N_5S$) C, H, N.

6-(*N*-Isopropyl)amidino-2-(*N*-(pyrimidin-2-yl)amino)benzothiazole Dihydrochloride (24). Beige powder was isolated (0.125 g, 41.1%), mp > 300 °C. IR (KBr) (ν_{max}/cm^{-1}): 3363, 3138, 1669, 1611. ^{1}H NMR (DMSO) (δ/ppm): 9.64 (d, 1H, J = 8.07 Hz, $H_{amidine}$), 9.50 (s, 1H, $H_{amidine}$), 9.20 (s, 1H, $H_{amidine}$), 8.76 (d, 2H, J = 4.8 Hz), 8.41 (s, 1H), 7.81 (d, 1H, J = 8.43 Hz), 7.74 (d, 1H, J = 8.49 Hz), 7.19 (t, 1H, J = 4.83 Hz), 5.89 (brs, 2H, NH_2^+), 4.19−4.09 (m, 1H, C$\underline{H}$), 1.29 (d, 6H, J = 6.24 Hz, $C\underline{H}_3$). ^{13}C NMR (DMSO) (δ/ppm): 162.70, 161.69, 158.20, 156.71, 152.53, 131.95, 126.19, 122.86, 122.25, 119.07, 115.25, 45.07, 21.29. Anal. ($C_{15}H_{18}Cl_2N_6S$) C, H, N.

6-Imidazolinyl-2-(*N*-(4-imidazolinylphenyl)amino)benzothiazole Dihydrochloride (25). Yellow powder was isolated (0.105 g, 34%), mp = 275−277 °C. IR (KBr) (ν_{max}/cm^{-1}): 3413, 3111, 2971, 1614. ^{1}H NMR (DMSO) (δ/ppm): 12.18 (brs, 1H, N$\underline{H}$), 10.67 (s, 4H, $H_{amidine}$), 8.55 (s, 1H), 8.03 (d, 2H, J = 8.82 Hz), 8.04 (d, 2H, J = 8.82 Hz), 7.95 (dd, 1H, J_1 = 8.46 Hz, J_2 = 1.2 Hz), 7.82 (d, 1H, J = 8.46 Hz), 3.92 (s, 4H, $C\underline{H}_2$), 3.70 (s, 4H, $C\underline{H}_2$). ^{13}C NMR (DMSO) (δ/ppm): 164.53, 164.39, 163.95, 155.91, 145.16, 131.11, 130.15, 126.68, 122.30, 119.76, 117.72, 116.00, 115.21, 44.26, 44.09. Anal. ($C_{19}H_{20}Cl_2N_6S$) C, H, N.

6-Imidazolinyl-2-(*N*-(3-methylpyridin-2-yl)amino)benzothiazole Dihydrochloride (26). White powder was isolated (0.12 g, 40.5%), mp > 300 °C. IR (KBr) (ν_{max}/cm^{-1}): 3413, 3098, 2967, 1629, 1611. ^{1}H NMR (DMSO) (δ/ppm): 10.76 (s, 2H, $H_{amidine}$), 8.70 (s, 1H), 8.29 (d, 1H, J = 4.68 Hz), 8.06 (d, 1H, J = 8.55 Hz), 7.78 (d, 1H, J = 8.55 Hz), 7.68 (d, 1H, J = 7.2 Hz), 7.07 (dd, 1H, J_1 = 7.12 Hz, J_2 = 5.11 Hz), 4.00 (s, 4H, $C\underline{H}_2$), 3.76 (brs, 2H, $N\underline{H}_2^+$), 2.39 (s, 3H, $C\underline{H}_3$). ^{13}C NMR (DMSO) (δ/ppm): 164.68, 163.40, 149.31, 143.08, 142.59, 139.55, 132.03, 126.41, 122.53, 120.98, 118.63, 118.08, 115.09, 44.20, 16.74. Anal. ($C_{16}H_{17}Cl_2N_5S$) C, H, N.

6-Imidazolinyl-2-(*N*-(4-methylpyridin-2-yl)amino)benzothiazole Dihydrochloride (27). White powder was isolated (0.12 g, 42.2%), mp > 300 °C. IR (KBr) (ν_{max}/cm^{-1}): 3423, 3051, 2941, 2690, 1653. ^{1}H NMR (DMSO) (δ/ppm): 10.71 (s, 2H, $H_{amidine}$), 8.64 (d, 1H, J_2 = 1.71 Hz), 8.21 (d, 1H, J = 4.98 Hz), 7.97 (dd,

1H, $J_1 = 8.52$ Hz, $J_2 = 1.71$ Hz), 7.71 (d, 1H, $J = 8.52$ Hz), 6.99 (s, 1H), 6.89 (d, 1H, $J = 4.98$ Hz), 4.13 (brs, 2H, $N\underline{H}_2^+$), 3.91 (s, 4H, $C\underline{H}_2$), 2.26 (s, 3H, $C\underline{H}_3$). ^{13}C NMR (DMSO) (δ/ppm): 164.54, 163.14, 153.75, 150.63, 150.29, 145.36, 132.08, 126.46, 122.61, 119.19, 119.05, 115.09, 111.88, 44.17, 20.80. Anal. ($C_{16}H_{17}Cl_2N_5S$) C, H, N.

6-Imidazolinyl-2-(*N*-(5-methylpyridin-2-yl)amino)benzothiazole Dihydrochloride (28). White powder was isolated (0.19 g, 67.1%), mp > 300 °C. IR (KBr) (ν_{max}/cm^{-1}): 3370, 3082, 2961, 1654, 1590. ^{1}H NMR (DMSO) (δ/ppm): 10.75 (s, 2H, $H_{amidine}$), 8.71 (d, 1H, $J = 1.38$ Hz), 8.25 (s, 1H), 8.04 (dd, 1H, $J_1 = 8.55$ Hz, $J_2 = 1.65$ Hz), 7.18 (d, 1H, $J = 8.37$ Hz), 4.23 (brs, 2H, $N\underline{H}_2^+$), 3.99 (s, 4H, $C\underline{H}_2$), 2.27 (s, 3H, $C\underline{H}_3$). ^{13}C NMR (DMSO) (δ/ppm): 164.68, 163.11, 154.02, 148.79, 145.68, 139.52, 132.11, 126.78, 126.39, 122.50, 118.90, 114.81, 111.41, 44.19, 17.22. Anal. ($C_{16}H_{17}Cl_2N_5S$) C, H, N.

6-Imidazolinyl-2-(*N*-(6-methylpyridin-2-yl)amino)benzothiazole Dihydrochloride (29). White powder was isolated (0.12 g, 41.4%), mp > 300 °C. IR (KBr) (ν_{max}/cm^{-1}): 3385, 2958, 2545, 1648 (C=N). ^{1}H NMR (DMSO) (δ/ppm): 10.67 (s, 2H, $H_{amidine}$), 8.62 (s, 1H), 7.97 (dd, 1H, $J_1 = 8.43$ Hz, $J_2 = 1.23$ Hz), 7.69 (d, 1H, $J = 8.52$ Hz), 7.63 (dd, 1H, $J_1 = 7.74$ Hz, $J_2 = 7.68$ Hz), 6.96 (d, 1H, $J = 8.04$ Hz), 6.86 (d, 1H, $J = 7.32$ Hz), 3.92 (s, 4H, $C\underline{H}_2$), 3.87 (brs, 2H, $N\underline{H}_2^+$), 2.46 (s, 3H, $C\underline{H}_3$). ^{13}C NMR (DMSO) (δ/ppm): 164.58, 163.03, 155.36, 153.90, 150.09, 138.86, 132.26, 126.38, 122.45, 118.96, 116.80, 114.82, 108.50, 44.18, 23.25. Anal. ($C_{16}H_{17}Cl_2N_5S$) C, H, N.

6-Imidazolinyl-2-(*N*-(5-chloropyridin-2-yl)amino)benzothiazole Dihydrochloride (30). Beige powder was isolated (0.14 g, 53.3%), mp > 300 °C. IR (KBr) (ν_{max}/cm^{-1}): 3411, 3090, 2893, 1625. ^{1}H NMR (DMSO) (δ/ppm): 10.75 (brs, 2H, $H_{amidine}$), 8.68 (d, 1H, $J_2 = 1.71$ Hz), 8.37 (d, 1H, $J = 2.46$ Hz), 7.98 (dd, 1H, $J_1 = 8.58$ Hz, $J_2 = 1.71$ Hz), 7.84 (dd, 1H, $J_1 = 8.82$ Hz, $J_2 = 2.46$ Hz), 7.70 (d, 1H, $J = 8.58$ Hz), 7.22 (d, 1H, $J = 8.76$ Hz), 4.64 (brs, 2H, $N\underline{H}_2^+$), 3.91 (s, 4H, $C\underline{H}_2$). ^{13}C NMR (DMSO) (δ/ppm): 164.51, 162.75, 153.74, 149.71, 144.70, 138.42, 132.03, 126.48, 123.81, 122.70, 119.18, 115.18, 113.20, 44.18. Anal. ($C_{15}H_{14}C_{l3}N_5S$) C, H, N.

6-Imidazolinyl-2-(*N*-(pyrimidin-2-yl)amino)benzothiazole Dihydrochloride (31). Beige powder was isolated (0.136 g, 48.9%), mp > 300 °C. IR (KBr) (ν_{max}/cm^{-1}): 3415, 3084, 2972, 1611, 1591. ^{1}H NMR (DMSO) (δ/ppm): 10.67 (s, 2H, $H_{amidine}$), 8.77−8.71 (m, 3H), 8.07 (dd, 1H, $J_1 = 8.60$ Hz, $J_2 = 1.75$ Hz), 7.84 (d, 1H, $J = 8.55$ Hz), 7.19 (t, 1H, $J = 4.83$ Hz), 4.03 (s, 4H, $C\underline{H}_2$), 3.48 (brs, 2H, $N\underline{H}_2^+$). ^{13}C NMR (DMSO) (δ/ppm): 158.61, 150.99, 144.87, 134.48, 133.14, 130.67, 126.87, 123.09, 120.17, 116.16, 115.93, 44.87. Anal. ($C_{14}H_{14}Cl_2N_6S$) C, H, N.

Antitumor Activity Assays. The HeLa, MCF-7, SW 620, MiaPaCa-2, Hep-2, H 460, and WI 38 cells were cultured as monolayers and maintained in DMEM supplemented with 10% FBS, 2 mM L-glutamine, 100 U/mL penicillin, and 100 μg/mL streptomycin in a humidified atmosphere with 5% CO_2 at 37 °C.

The growth inhibition activity was assessed as described previously, according to the slightly modified procedure of the National Cancer Institute, Developmental Therapeutics Program. The cells were inoculated onto standard 96-well microtiter plates on day 0 at 3×10^3 to 6×10^3 cells/well, depending on the doubling times of specific cell line. Test agents were then added in five consecutive 10-fold dilutions (10^{-8}−10^{-4} mol/L) and incubated for a further 72 h. Working dilutions were freshly prepared on the day of testing. The solvent (DMSO) was also tested for eventual inhibitory activity by adjusting its concentration to be the same as the working concentrations (maximal concentration of DMSO was 0.25%). After 72 h of incubation, the cell growth rate was evaluated by performing the MTT assay,[33,34] which detects dehydrogenase activity in viable cells. The absorbance (OD) was measured on a microplate reader at 570 nm.

Each test point was performed in quadruplicate in three individual experiments. The results are expressed as IC_{50}, which is the concentration necessary for 50% of inhibition. The IC_{50} values for each compound are calculated from dose−response curves using linear regression analysis by fitting the test concentrations that give PG values above and below the reference value (i.e. 50%). Each result is the mean value from three separate experiments.

Cell Cycle Analysis. The 2×10^5 cells were seeded per well in a six-well plate. After overnight incubation, tested compounds were added. After the desired length of time, the attached cells were trypsinized, combined with floating cells, washed with PBS, and fixed with 70% ethanol. Immediately before analysis, the cells were washed with PBS and incubated with 0.2 μg/μL RNase A at 37 °C for 15 min. Subsequently, cells were stained with 50 μg/mL of propidium iodide (PI) and analyzed by Becton Dickinson FACSCalibur flow cytometer. For each analysis, 20000 events were measured. Measurements were performed in duplicate for two independent experiments. The percentage of the cells in each cell cycle phase was based on the obtained DNA histograms and determined using the ModFit LT software (Verity Software House).

Detection of Apoptosis. Annexin-V Assay. Detection and quantification of apoptotic cells at the single cell level were performed by staining the cells with annexin-V Alexa Fluor 488 conjugate (Molecular Probes, Invitrogen) and 7-aminoactinomycin D (7-AAD, Invitrogen). The 2×10^5 cells were seeded per well into a six-well plate and analyzed on a FACSCalibur flow cytometer (Becton Dickinson, San Jose, CA). The tested compounds were added to the attached cells at various concentrations (as shown in the results section). After the desired length of time, both floating and attached cells were collected. The cells were then washed with annexin-V binding buffer (10 mM HEPES, 140 mM NaCl, 2.5 mM $CaCl_2$, pH 7.4), pelleted, and incubated for 20 min in staining solution (annexin-V Alexa Fluor 488 conjugate and 1 μg/mL 7-AAD in annexin-V binding buffer). The cells were then run on a flow cytometer and analyzed in Summit software (Cytomation Inc., CO). Annexin-V positive cells were determined to be apoptotic, and double positive cells (both annexin-V and 7-AAD) were determined to be necrotic.

Principal Components and Partial Least Square Analysis. Smile codes of the molecules were used as input for the program Volsurf.[32,35] Volsurf utilizes information from the molecular interaction fields (MIF) determined by GRID[36] to calculate a series of physicochemically relevant molecular descriptors.

For each MIF the interaction energy between a molecule of known three-dimensional structure ("target"), generated by Volsurf, and a small chemical group ("probe") was computed for a set of positions of the probe around the target. Probes that mimic functional groups that may be present in a protein (e.g., receptor or transporter) active site (H_2O, $-NH_2^+$, $-CH_3$, O, and DRY probe) were selected. For each probe thousands of interaction energies were calculated at the nodes of the regular three-dimensional grid around the target. Volsurf used calculated MIFs to derive a series of 126 scalar descriptors that describe molecular size, shape, solubility, distribution of hydrophilic and hydrophobic regions, lipophilicity, flexibility, and presence/distribution of pharmacophoric descriptors. Besides describing pharmacokinetic processes,[37] Volsurf has been used to also describe ligand−protein interactions and antibacterial activity.[38,39]

In order to determine most variable descriptors (*X*-variables) within the set of compounds and the compounds distribution in the space of the descriptors, we conducted principal components (PC) analysis. Further, to derive the relationship between several most relevant *X*-variables and the measured inhibition, we performed partial least-squares (PLS) statistical analysis. In this way, we derived QSAR models that connect physicochemical molecular descriptors with the specific response of certain cell line. The predictivity of the models was evaluated by using "internal validation", by means of standard leave-one-out (LOO) analysis.

Acknowledgment. Support for this study by the Ministry of Science, Education and Sport of Croatia is gratefully acknowledged (Projects 125-0982464-1356, 098-0982464-

2514, 098-0982464-2393, 098-1191344-2860, and 119-119307-1332).

Supporting Information Available: Experimental and spectroscopic data for cyano derivatives **1**−**6** and **11**−**17** with the reference list, elemental analysis results of novel compounds, X-ray crystal structure analysis results, and selected crystallographic data for compound **15**. This material is available free of charge via the Internet at http://pubs.acs.org. The CCDC number 709670 for compound **15** contains the supplementary crystallographic data for this paper. These data can be obtained free of charge at www.ccdc.cam.ac.uk/conts/retrieving.html [or from the Cambridge Crystallographic Data Centre (CCDC), 12 Union Road, Cambridge CB2 1EZ, U.K.; fax, +44(0)1223-336033; e-mail, deposit@ccdc.cam.ac.uk]. A table of structure factors is available from the authors.

References

(1) Hanahan, D.; Weinberg, R. A. The Hallmarks of Cancer. *Cell* **2000**, *100*, 57–70.

(2) Gibbs, J. B. Mechanism-Based Target Identification and Drug Discovery in Cancer Research Science. *Science* **2000**, *287*, 1969–1973.

(3) Brana, M. F.; Cacho, M.; Gradillas, A.; Pascual-Teresa, B.; Ramos, A. Intercalators as Anticancer Drugs. *Curr. Pharm. Des.* **2001**, *7*, 1745–1780.

(4) Norton, J. T.; Witschi, M. A.; Luong, L.; Kawamura, A.; Ghosh, S.; Stack, M. S.; Sim, E.; Avram, M. J.; Appella, D. H.; Huang, S. Synthesis and Anticancer Activities of 6-Amino Amonafide Derivatives. *Anti-Cancer Drugs* **2008**, *19*, 23–36.

(5) Damia, G.; Broggini, M. DNA Minor Groove Binding Agents. *Drugs Future* **2005**, *30*, 301–309.

(6) Matsuba, Y.; Edatsugi, H.; Mita, I.; Matsunaga, A.; Nakanishi, O. A Novel Synthetic DNA Minor Groove Binder, MS-247: Antitumor Activity and Cytotoxic Mechanism. *Cancer Chemother. Pharmacol.* **2000**, *46*, 1–9.

(7) Keating, G. M.; Jarvis, B. Letrozole: An Updated Review of Its Use in Postmenopausal Women with Advanced Breast Cancer. *Am. J. Cancer* **2002**, *1*, 351–371.

(8) Pandey, R.; Patil, N.; Rao, M. Proteases and Protease Inhibitors: Implications in Antitumorigenesis and Drug Development. *Int. J. Hum. Genet.* **2007**, *7*, 67–82.

(9) Ban, M.; Taguchi, H.; Katsushima, T.; Takahashi, M.; Shinoda, K.; Watanabe, A.; Tominaga, T. Novel Antiallergic and Antiinflammatory Agents. Part I: Synthesis and Pharmacology of Glycolic Amide Derivatives. *Bioorg. Med. Chem.* **1998**, *6*, 1069–1076.

(10) Papadopoulou, C.; Geronikaki, A.; Hadjipavlou-Litina, D. Synthesis and Biological Evaluation of New Thiazolyl/benzothiazolyl-amides, Derivatives of 4-Phenyl-piperazine. *Farmaco* **2005**, *60*, 969–973.

(11) Chung, Y.; Shin, Y.-K.; Zhan, C.-G.; Lee, S.; Cho, H. Synthesis and Evaluation of Antitumor Activity of 2- and 6-[(1,3-Benzothiazol-2-yl)aminomethyl]-5,8-dimethoxy-1,4-naphthoquinone Derivatives. *Arch. Pharmacal Res.* **2004**, *27*, 893–900.

(12) McFadyen, M. C. E.; Melvin, W. T.; Murray, G. I. Cytochrome *P*450 Enzymes: Novel Options for Cancer Therapeutics. *Mol. Cancer Ther.* **2004**, *3*, 363–371.

(13) Yoshida, M.; Hayakawa, I.; Hayashi, N.; Agatsuma, T.; Oda, Y.; Tanzawa, F.; Iwasaki, S.; Koyama, K.; Furukawa, H.; Kurakata, S. Synthesis and Biological Evaluation of Benzothiazole Derivatives as Potent Antitumor Agents. *Bioorg. Med. Chem. Lett.* **2005**, *15*, 3328–3332.

(14) Starčević, K.; Ćaleta, I.; Cinčić, D.; Kaitner, B.; Kralj, M.; Ester, K.; Karminski-Zamola, G. Synthesis, Crystal Structure Determination and Antiproliferative Evaluation of Novel Benzazoyl Benzamides. *Heterocycles* **2006**, *68*, 2285–2299.

(15) Baell, J. B.; Forsyth, S. A.; Gable, R. W.; Norton, R. S.; Mulder, R. J. Design and Synthesis of Type-III Mimetics of ω-Conotoxin GVIA. *J. Comput.-Aided Mol. Des.* **2002**, *15*, 1119–1136.

(16) Westway, S. M.; Thompson, M.; Rami, H. K.; Stemp, G.; Trouw, L. S.; Mitchell, D. J.; Seal, J. T.; Medhurst, S. J.; Lappin, S. C.; Biggs, J.; Wright, J.; Arpino, S.; Jerman, J. C.; Cryan, J. E.; Holland, V.; Winborn, K. Y.; Coleman, T.; Stevens, A. J.; Davis, J. B.; Gunthorpe, M. J. Design and Synthesis of 6-Phenylnicotinamide Derivatives as Antagonists of TRPV1. *Bioorg. Med. Chem. Lett.* **2008**, *18*, 5609–5613.

(17) Das, J.; Lin, J.; Moquin, R. V.; Shen, Z.; Spergel, S. H.; Wityak, J.; Doweyko, A. M.; DeFex, H. F.; Fang, Q.; Pang, S.; Pitt, S.; Ren Shen, D.; Schieven, G. L.; Barrish, J. C. Molecular Design, Synthesis, and Structure−Activity Relationships Leading to the Potent and Selective P56^{lck} Inhibitor BMS-243117. *Bioorg. Med. Chem. Lett.* **2003**, *13*, 2145–2149.

(18) Das, J.; Moquin, R. V.; Lin, J.; Liu, C.; Doweyko, A. M.; DeFex, H. F.; Fang, Q.; Pang, S.; Pitt, S.; Ren Shen, D.; Schieven, G. L.; Barrish, J. C.; Wityak, J. Discovery of 2-Amino-heteroaryl-benzothiazole-6-anilides as Potent p56^{lck} Inhibitors. *Bioorg. Med. Chem. Lett.* **2003**, *13*, 2587–2590.

(19) Gaillard, P.; Jeanclaude-Etter, I.; Ardissone, V.; Arkinstall, S.; Cambet, Y.; Camps, M.; Chabert, C.; Church, D.; Cirillo, R.; Gretener, D.; Halazy, S.; Nichols, A.; Szyndralewiez, C.; Vitte, P.-A.; Gotteland, J.-P. Design and Synthesis of the First Generation of Novel Potent, Selective, and in Vivo Active (Benzothiazol-2-yl)acetonitrile Inhibitors of the c-Jun N-Terminal Kinase. *J. Med. Chem.* **2005**, *48*, 4596–4607.

(20) Liu, C.; Lin, J.; Pitt, S.; Zhang, R. F.; Sack, J. S.; Kiefer, S. E.; Kish, K.; Doweyko, A. M.; Zhang, H.; Marathe, P. H.; Trzaskos, J.; Mckinnon, M.; Dodd, J. H.; Barrish, J. C.; Schieven, G. L.; Leftheris, K. Benzothiazole Based Inhibitors of p38a MAP Kinase. *Bioorg. Med. Chem. Lett.* **2008**, *18*, 1874–1879.

(21) Pinar, A.; Yurdakul, P.; Yildiz, I.; Temiz-Arpaci, O.; Acan, N. L.; Aki-Sener, E.; Yalcin, I. Some Fused Heterocyclic Compounds as Eukaryotic Topoisomerase II Inhibitors. *Biochem. Biophys. Res. Commun.* **2004**, *317*, 670–674.

(22) Abdel-Aziz, M.; Matsuda, K.; Otsuka, M.; Uyeda, M.; Okawara, T.; Suzuki, K. Inhibitory Activities against Topoisomerase I & II by Polyhydroxybenzoyl Amide Derivatives and Their Structure−Activity Relationship. *Bioorg. Med. Chem. Lett.* **2004**, *14*, 1669–1672.

(23) Njar, V. C. O.; Gediya, L.; Purushottamachar, P.; Chopra, P.; Vasaitis, T. S.; Khandelwal, A.; Mehta, J.; Huynh, C.; Belosay, A.; Patel, J. Retinoic Acid Metabolism Blocking Agents (RAMBAs) for Treatment of Cancer and Dermatological Diseases. *Bioorg. Med. Chem.* **2006**, *14*, 4323–4340.

(24) Wang, Y.; Serradell, N. R-115866. Retinoic Acid Metabolism-Blocking Agent, Treatment of Psoriasis, Treatment of Acne. *Drugs Future* **2007**, *32*, 1040–1045.

(25) Sawhney, S. N.; Boykin, D. W. Transmission of Substitutent Effects in Heterocyclic Systems by Carcon-13 Nuclear Magnetic Resonance. Benzothiazoles. *J. Org. Chem.* **1979**, *44*, 1136–1142.

(26) Ćaleta, I.; Cetina, M.; Hergold-Brundić, A.; Nagl, A.; Karminski-Zamola, G. Synthesis and Crystal Structure Determination of 6-(*N*-Isopropyl)amidino-2-methylbenzothiazole Hydrochloride Monohydrate and 2-(Amino-6-(*N*-isopropyl)amidinobenzothiazole Hydrochloride. *Struct. Chem.* **2003**, *14*, 585–592.

(27) Jarak, I.; Kralj, M.; Šuman, L.; Pavlović, G.; Dogan Koružnjak, J.; Piantanida, I.; Žinić, M.; Pavelić, K.; Karminski-Zamola, G. Novel Cyano- and *N*-Isopropylamidino-Substituted Derivatives of Benzo[*b*-]thiophene-2-carboxanilides and Benzo[*b*]thieno[2,3-*c*]quinolones: Synthesis, Photochemical Synthesis, Crystal Structure Determination and Antitumor Evaluation. Part 2. *J. Med. Chem.* **2005**, *48*, 2346–2360.

(28) Farley, T. A.; Tidwell, R. R.; Donkor, I.; Naiman, N. A.; Ohemeng, K. A.; Lomberdy, R. J.; Bentley, J. A.; Cory, M. Structure, DNA Minor Groove Binding, and Base Pair Specificity of Alkyl- and Aryl-Linked Bis(amidinobenzimidazoles) and Bis(amidinoindoles). *J. Med. Chem.* **1993**, *36*, 1746–1753.

(29) Farrugia, L. J. ORTEP-3 for Windows. *J. Appl. Crystallogr.* **1997**, *30*, 565.

(30) Ćaleta, I.; Cinčić, D.; Karminski-Zamola, G.; Kaitner, B. The Synthesis and Structure of Two Novel *N*-(Benzothiazol-2-yl)benzamides. *J. Chem. Crystallogr.* **2008**, *38*, 775–780.

(31) Serafim, T. L.; Oliveira, P. J.; Sardao, V. A.; Perkins, E.; Parke, D.; Holy, J. Different Concentrations of Berberine Result in Distinct Cellular Localization Patterns and Cell Cycle Effects in a Melanoma Cell Line. *Cancer Chemother. Pharmacol.* **2008**, *61*, 1007–1018.

(32) Cruciani, G.; Crivori, P.; Carrupt, P.-A.; Testa, B. Molecular fields in quantitative structure−permeation relationships: the VolSurf approach. *J. Mol. Struct.: THEOCHEM* **2000**, *503*, 17–30.

(33) Hranjec, M.; Kralj, M.; Piantanida, I.; Sedić, M.; Šuman, L.; Pavelić, K.; Karminski-Zamola, G. Novel Cyano- and Amidino-Substituted Derivatives of Styryl-2-Benzimidazoles and Benzimidazo[1,2-*a*]quinolines. Synthesis, Photochemical Synthesis, DNA Binding and Antitumor Evaluation, Part 3. *J. Med. Chem.* **2007**, *50*, 5696–5711.

(34) Hranjec, M.; Piantanida, I.; Kralj, M.; Šuman, L.; Pavelić, K.; Karminski-Zamola, G. Novel Amidino-Substituted Thienyl- and Furylvinyl-benzimidazole Derivatives and Their Photochemical Conversion into Corresponding Diaza-cyclopenta[*c*]fluorenes. Synthesis, Interactions with DNA and RNA and Antitumor Evaluation. *J. Med. Chem.* **2008**, *51*, 4899–4910.

(35) Cruciani, G.; Pastor, M.; Guba, W. VolSurf: A New Tool for Pharmacokinetic Optimization of Lead Compounds. *Eur. J. Pharm. Sci.* **2000**, *11*, S29–S39.

(36) Goodford, P. J. Computational Procedure for Determining Energetically Favorable Binding Sites on Biologically Important Macromolecules. *J. Med. Chem.* **1985**, *28*, 849–857.

(37) Bertoša, B.; Kojić-Prodić, B.; Ramek, M.; Piperaki, S.; Tsantili-Kakoulidou, A.; Wade, R.; Tomić, S. A New Approach To Predict

the Biological Activity of Molecules Based on Similarity of Their Interaction Fields and the logP and logD Values: Application to Auxins. *J. Chem. Inf. Comput. Sci.* **2003**, *43*, 1532–1541.
(38) Cianchetta, G.; Mannhold, R.; Cruciani, G.; Baroni, M.; Cecchetti, V. Chemometric Studies on the Bactericidal Activity of Quinolones via an Extended VolSurf Approach. *J. Med. Chem.* **2004**, *47*, 3193–3201.
(39) Zamora, I.; Oprea, T.; Cruciani, G.; Pastor, M.; Ungell, A. L. Surface Descriptors for Protein−Ligand Affinity Prediction. *J. Med. Chem.* **2003**, *46*, 25–33.

JM801566Q